Tracing the Uncertain Chinese Mercury Footprint within the Global Supply Chain Using a Stochastic, Nested Input−Output Model

Haoran Zhang,[†,‡,§] Kehan He,[†,§] Xuejun Wang,*[,‡] and Edgar G. Hertwich*[,†]

[†]Center for Industrial Ecology, School of Forestry and Environmental Studies, Yale University, New Haven, Connecticut 06511, United States

[‡]Ministry of Education Laboratory of Earth Surface Process, College of Urban and Environmental Sciences, Peking University, Beijing 100871, China

Ⓢ *Supporting Information*

ABSTRACT: A detailed understanding of the mercury footprint at subnational entity levels can facilitate the implementation of the "Minamata Convention on Mercury", especially for China, the largest mercury emitter worldwide. Some provinces of China have more than 100 million people, with economic activities and energy consumption levels comparable to those of smaller G7 countries. We constructed a stochastic, nested multiregion input−output (MRIO) model, which regionalized the China block in the EXIOBASE global-scale MRIO table, to model the mercury footprint associated with global supply chains spanning China's regions and other countries. The results show that Tianjin, Shanghai, and Ningxia had the highest per capita mercury footprint in China, which was comparable to the footprint of Australia and Norway and exceeded the footprint of most other countries. Some developed regions in China (e.g., Guangdong, Jiangsu) had higher mercury final product-based inventories (FBI) and consumption-based inventories (CBI) than production-based inventories (PBI), emphasizing the role of these regions as centers of both consumption and economic control. Uncertainties of Chinese provincial mercury footprint varied from 8% to 34%. Our research also revealed that international and inter-regional final product and intermediate product trades reshape the mercury emissions of Chinese provinces and other countries to a certain extent.
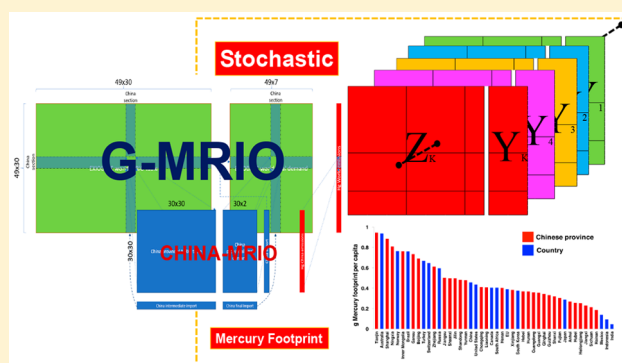
1. INTRODUCTION

Resource and environmental issues are in the global dimension, with supply chains spanning various countries and regions.[1−3] The rising anthropic pressures on the environment require robust indicators for policy makers to measure anthropic pressures not only locally but also in other regions.[4,5] Recent studies have revealed that the consumption of products and services is the underlying driver of resource exploitation and environmental pollution beyond ecological limits.[6] Hence, the urge to allocate environmental impact responsibilities to consumers has led to the formulation of consumption-based indicators, often denoted as "footprints", to illustrate the impacts of the consumption of goods and services in the entire supply chain.[7,8] Footprint indicators are utilized as metrics to assess the anthropic pressures caused by final domestic demands and their consequent exterritorial environmental impacts at different scales and to analyze policy-relevant issues such as carbon emission leakage, virtual water, material use, and the distribution of air pollution among countries and regions based on environmentally extended multiregion input−output models (EE-MRIO).[9−16] Via the employment of economic and trade data at multiple stages, EE-MRIO models can allocate direct and indirect upstream anthropic pressures to final demand.[17,18] The use of EE-MRIO models is becoming the prevailing approach of researchers, organizations, and governments to estimate footprint indicators.[19]

Similar to other footprint indicators, the "mercury footprint" has been put forward to identify the impacts of national or regional consumption behaviors on mercury emissions.[20] Mercury is a critical toxic and global pollutant that can cause severe damages to ecosystems and human health.[21,22] Considering the adverse effects of mercury, the "Minamata Convention on Mercury" to control mercury emissions globally has been signed by 140 nations in 2013.[23] Understanding the mercury footprint provides a crucial knowledge base for governments and policy makers to fulfill their obligations under the "Minamata Convention on Mercury".[20] China is the largest emitter of global anthropogenic atmospheric mercury and contributes approximately 27% of the global total emissions.[24] Considering China's role as a main

producer and consumer in the world economy, comprehensive knowledge of the Chinese mercury footprint can help the Chinese government better implement the Convention. Liang et al. calculated the atmospheric mercury footprints of nations based on global MRIO tables from the World Input−Output Database (WIOD) and discussed upstream production, downstream production, and consumption roles in global mercury emissions.[20] Li et al. used a MRIO table for 2010 with 186 individual economies and 26 sectors from the Eora database to trace embodied mercury emissions flowing worldwide.[25] Liang et al. compiled a bottom-up mercury emission inventory of China in 2007 and used the Chinese 2007 MRIO table to calculate the Chinese virtual mercury emissions network.[26] Hui et al. modeled mercury flows in China's production system and linked the substance flow analysis (SFA) method with the EE-MRIO model to uncover global consumption drivers of Chinese mercury flows.[27] Chen et al. combined the 2010 Chinese MRIO model with an atmospheric transport model to simulate the atmospheric mercury deposition embodied among Chinese regions.[28]

The above-mentioned studies mainly calculated the Chinese or global mercury footprint based on a single global-scale MRIO table or a Chinese province-scale MRIO table. We believe the calculation of the mercury footprint at the global scope using a global-scale MRIO database (e.g., Eora,[29,30] EXIOBASE,[31] GTAP,[32] WIOD,[33] and GRAM[34,35]) can reveal all Chinese mercury emissions driven by production and consumption activities in global supply chains.[36] However, as a country with vast territory and population, China possesses high spatial heterogeneity in resource uses and pollution emissions.[37] Some provinces (e.g., Shandong, Jiangsu) have populations of more than 100 million, and the economic activities and energy consumption of these provinces are equivalent to or even more than those of some large countries. In the conventional global-scale MRIO tables, China is always treated as a whole. This approach ignores the different performances of mercury footprints among Chinese provinces. In contrast, the use of a Chinese province-scale MRIO table could enable the calculation of the mercury footprint associated with domestic supply chains and interprovincial trading but fail to distinguish the range of technologies employed to produce international exports and imports. Previous studies could not uncover the impacts of Chinese provinces' production and consumption activities on global mercury emissions.[38] Since it is necessary to formulate local demand-based mercury control policies that reflect influences on the mercury emissions of other regions throughout global supply chains,[39,40] a study addressing this topic is essential.

To illustrate and understand the local Chinese provincial mercury footprint from a global perspective, multiscale nested MRIO tables should be applied. Recently, Wang et al. developed a nested Chinese MRIO table inputting 30 Chinese provinces into an international MRIO framework.[41] Liu et al. used a 2007 Chinese MRIO table to disaggregate the Chinese region in GTAP into 30 subregions.[42] Meanwhile, MRIO based footprint analysis lack uncertainty estimation in most previous studies. We considered it vital to better understand the uncertain Chinese mercury footprint.[43] In this study, we nested a Chinese nation-scale MRIO table into the global-scale MRIO table from EXIOBASE database updated as of the year 2010. Applying Monte Carlo simulation, we extended the nested MRIO into stochastic forms and provided an estimation of the uncertainty associated with Chinese mercury footprint

along with a comparison with different data sources. Our analysis provides comprehensive answers to the following questions:

(a) What is the performance of each Chinese province's mercury footprint within the entire global supply chain?
(b) Where are the origins and destinations of mercury emissions embodied in international trade between each Chinese province and other countries?
(c) What is the tolerance of our result against uncertainty?

2. MATERIALS AND METHODS

2.1. Emissions Embodied in Trade and Emission Inventories. A common, territorial, or production-based emissions inventory (PBI) describes the emissions of a pollutant within a specific region or nation. A consumption-based inventory (CBI) describes the emissions associated with the production of products consumed in a specific region, taking the life-cycle impact of these products into account.[44] We also define a final product-based inventory (FBI) as the cradle-to-gate emissions associated with the final products produced in a region.[45] The difference between these inventories is the emissions embodied in the trade of intermediate and final products. CBI and FBI are calculated using a MRIO table.[46]

A MRIO table consists of a section $\mathbf{Z}$ describing the trade in intermediate products among region-sectors, a section $\mathbf{Y}$ describing the final consumption of products, and a section $\mathbf{V}$ describing the use of factors of production (value added, resources, emissions). Diagonal blocks $\mathbf{Z}^{R,R}$ and $\mathbf{Y}^{R,R}$ describe the use of domestic products as intermediate products (for domestic production) and as final products (for domestic final consumption), respectively. Off-diagonal blocks $\mathbf{Z}^{S,R}$ and $\mathbf{Y}^{S,R}$ describe the inter-regional trade of intermediate and final products, respectively.[47]

When the matrices describing the input of production factors and intermediate inputs are normalized by the production volumes of each production activity, we get coefficient matrices $\mathbf{S}$ and $\mathbf{A}$, respectively, which describe the inputs used to produce one unit of output. These matrices can be used to calculate the multiplier, an expression of the production factors required to produce a unit of final output (cradle-to-gate), using the Leontief inverse.[48]

$$m = S(I - A)^{-1} \tag{1}$$

The mercury emissions embodied in the trade of final and intermediate products[49] are
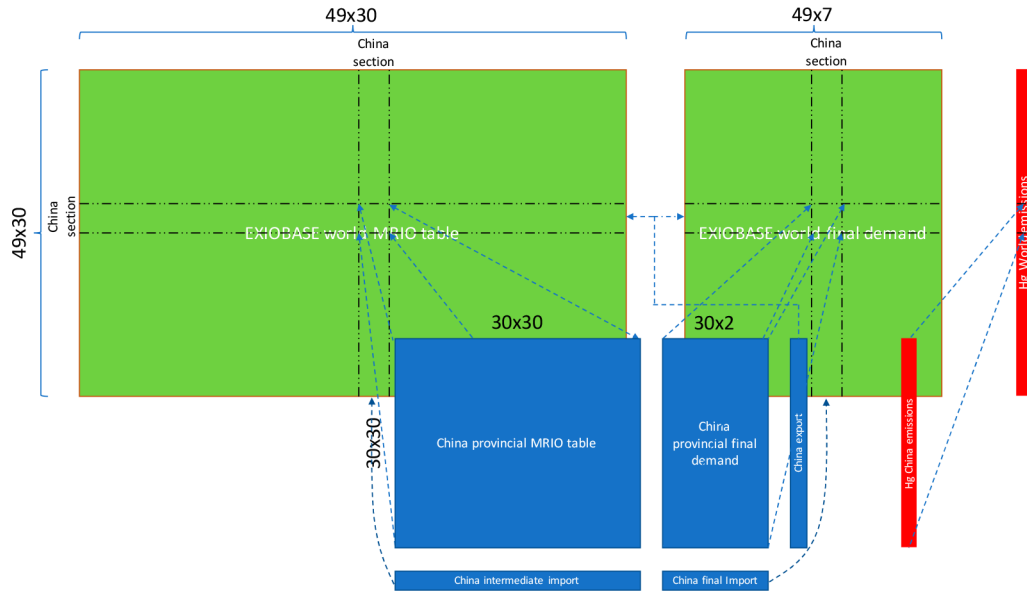
$$EEFI^R = \sum_{S \neq R} m^S Y^{S,R} \tag{2}$$

$$EEFX^R = \sum_{S \neq R} m^R Y^{R,S} \tag{3}$$

$$EEII^R = \sum_{S \neq R} m^S Z^{S,R} \tag{4}$$

$$EEIX^R = \sum_{S \neq R} m^R Z^{R,S} \tag{5}$$

where EEFI represents the emissions embodied in the import of final products, EEFX represents the emissions embodied in the export of final products, EEII represents the emissions embodied in the import of intermediate products, and EEIX

Figure 1. Regionalization of the China block in the EXIOBASE global-scale MRIO table by the Chinese subnational (30 sectors and 30 provinces) MRIO table.

represents the emissions embodied in the export of intermediate products.

The production-based inventory is simply given by $\mathrm{PBI}^R = \sum_R F^R$. The final product-based inventory is hence the production-based inventory minus the embodied emissions:[50]

$$\mathrm{FBI}^R = \mathrm{PBI}^R + \mathrm{EEII}^R - \mathrm{EEIX}^R = \sum_S m^R Y^{R,S} \quad (6)$$

$$\mathrm{CBI}^R = \mathrm{FBI}^R + \mathrm{EEFI}^R - \mathrm{EEFX}^R = \sum_S m^S Y^{S,R} \quad (7)$$

2.2. Building the Nested China-Global MRIO Table. The environmentally extended multiregional input−output model (EE-MRIO) has been widely used for analyzing the environmental footprint and embodied emissions in trade.[51,52] As described above, we need a nested China-global MRIO table to construct a spatially explicit assessment of the detailed Chinese mercury footprint within global supply chains.[1] Previous studies have provided us with a methodology reference for nesting the China national MRIO table into the global MRIO table.[41] Version 3.3 of EXIOBASE[53] was used in this work as the source of global-scale MRIO tables and environmental satellite data for mercury emissions of all countries and regions. The last updated and publicly available year for EXIOBASE database is 2011. Thus, we chose the Chinese MRIO table for the year of 2010 developed by the Institute of Geographic Sciences and Natural Resources Research, CAS,[54] to construct our nested model. CAS MRIO table has been widely used in existing footprint researches, so we assume its validity in the study to be conducted.

The intermediate and final trades in the Chinese national-scale MRIO table with provincial specifications were disaggregated into the global-scale MRIO table proportionally to Chinese exports and imports to other economies.[41,42] EXIOBASE 3.3 provided a global-scale MRIO table, and corresponding environmental satellite accounts were given in 200 sectors. Concordance had to be made to reduce the sector resolution to 30 sectors before the nesting process. Because

only two categories, namely, final consumption and capital formation, were given in the 2010 Chinese national-scale MRIO table, we also disaggregated the final demand in the Chinese national-scale MRIO table according to the final demand proportions for China in the EXIOBASE 3.3 MRIO table. Illustrative figures are given in Figure 1 to describe the nesting process. The nested processing and concordance matrix details are given in Supporting Information (SI, Text S1).

To increase data accuracy, we used the 2010 mercury emission data inventory of the Arctic Monitoring and Assessment Programme/United Nations Environment Programme (AMAP/UNEP)[21] to adjust the global mercury satellite data in the EXIOBASE 3.3. We used 30-province and 30-sector Chinese MRIO tables for the year 2010, which were published by Liu et al., as the Chinese national-scale MRIO data source in this study.[54] The direct mercury emission inventories of 30 Chinese provinces and 30 sectors in 2010 were taken from the study of Chen et al.[28]

2.3. Uncertainty Estimation. Due to limitations of data availability and computational power, formal analyses of uncertainty is not yet routine in footprint studies.[55,56] With reference to uncertainty simulation method developed by Lenzen et al.[43] we extended the nested MRIO into stochastic forms and provide an estimation of the uncertainty associated with Chinese mercury footprint. For each element of the source data x, definition of the order of magnitude of x as $\log_{10}(x)$. The absolute standard deviation of x is dx, so the relative standard deviation (RSD) is given as follows:
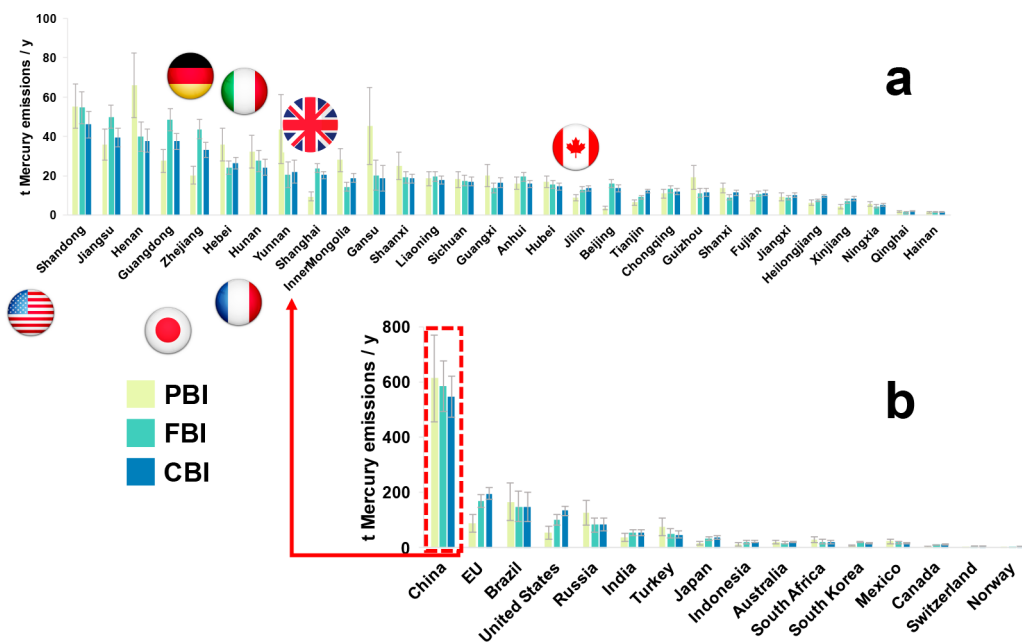
$$Rx = dx/x \quad (8)$$

Thus, the absolute error for the order of magnitude of x can be approximated as follows:

$$d(\log_{10} x) \approx \log_{10}(x + dx) - \log_{10} x = \log_{10}\left(\frac{x + dx}{x}\right) = \log_{10}(1 + Rx) \quad (9)$$

Then, we can obtain

$$\log_{10} x^{\times} = \log_{10} x + d(\log_{10} x) \quad (10)$$

C

Figure 2. Mercury emission inventories under three different allocation principles within the global dimension. PBI = production-based mercury inventories, FBI = final product-based mercury inventories, and CBI = consumption-based mercury inventories. (a) Chinese mercury inventories for 30 provinces within global supply chains. (b) Mercury inventories of global countries and regions within global supply chains. The error bars represent confidence intervals of width 2σ ($\pm$2SD, 95% of all observations).

Hence, the Monte Carlo perturbations can be conducted. In this approach, all uncertainties expressed by SDs refer to the logarithmic form of the parameter variables, since we assume the observations of MRIO entries are distributed log-normally.[57−59] By conducting Monte Carlo simulation for the error-adjusted input data, a large sample of K realizations of output results are generated. Then the K realizations are used to obtain and specify the underlying probability distributions of output results.

Concretely, we perturbed the entries of the nested MRIO coefficient $Z \rightarrow Z^{\times} = Z \otimes 10^{\delta Z}$, $Y \rightarrow Y^{\times} = Y \otimes 10^{\delta Y}$, and direct mercury emissions $F \rightarrow F^{\times} = F \otimes 10^{\delta F}$. Here, δx denoted a vector of stochastic variables distributed normally around zero-mean with SDs of parameter $d(\log_{10} x)$; the symbol $\otimes$ denoted the element-wise multiplication. The perturbed X is the sum of the perturbed Z and Y, $X^{\times} = Z^{\times} + Y^{\times}$, so as to obtain a balanced perturbed table. Also, the perturbation of X exceeding 3% threshold was discarded to avoid over pertabation.[57,58] Then, these perturbed realizations were substituted into Monte Carlo simulations to calculate the perturbed mercury footprint:

$$C^{\times} = (F^{\times}\hat{X}^{-1\times})(I - A^{\times})^{-1}Y^{\times} = (F^{\times}\hat{X}^{-1\times})(I - (Z^{\times}\hat{X}^{-1\times}))^{-1}Y^{\times} \quad (11)$$

By conducting the calculation for 10 000 iterations with stochastically simulated errors, the aggregated metrics for the underlying probability distribution functions were obtained as follows:

$$\mu_{C^{\times}} = \sum_{K} C^{\times}(k)/K \quad (12)$$

$$\sigma_{dc^{\times}} = \sqrt{\sum_{k} (C^{\times}(k) - \mu_{C^{\times}})^2 / K} \quad (13)$$

where K is 10 000 as iterator of the sample set; $\mu_{C^{\times}}$ is the mean and $\sigma_{dc^{\times}}$ is the standard deviations (SDs).

Second, for global-level mercury emission data, we used AMAP/UNEP national emission data to adjust for emission-factor based mercury emission inventory given in EXIOBASE. For Chinese provincial-level mercury emissions, the data were taken from the study of Chen et al.[28] Relevant calculation of uncertainty for the direct mercury data were given in SI (Text S3). Due to unavailable uncertainty information for the raw data used to construct the nested MRIO table, regression techniques, and error propagation algorithm developed by Lenzen et al. were employing to estimate SDs of MRIO table points.[29,41,43]

Lastly, since there are different databases of global-level MRIO and Chinese provincial-level MRIO tables, uncertainties may also be caused by the choice of data sources. A summary of the MRIO data sources is given in Table S1. In addition, the uncertainties associated with the choice of Chinese MRIO were also estimated and discussed in this study. A comparison of the difference in magnitude of emission multipliers is also conducted to assess the robustness of the nested MRIO against results obtained using other Chinese MRIO tables. Detailed descriptions of methodology used for uncertainty analysis are contained in the SI (Text S3).

3. RESULTS AND DISCUSSION

3.1. Production, Consumption, and Final Product Based Inventories of Mercury Emission. Figure 2 shows the mercury emission inventories under three different allocation principles in 2010 within the global dimension. China directly emitted 613t of atmospheric mercury in 2010 (PBI), contributing 32% of the total global mercury emissions. The total mercury FBI and CBI of China were 584t and 547 t, accounting for 30% and 28%, respectively, of the global total mercury emissions and were 4.8% and 11% lower, respectively, than the mercury PBI of China. The detailed Chinese provincial mercury inventories under three accounting frameworks within global supply chains are depicted in Figure 2a. Of
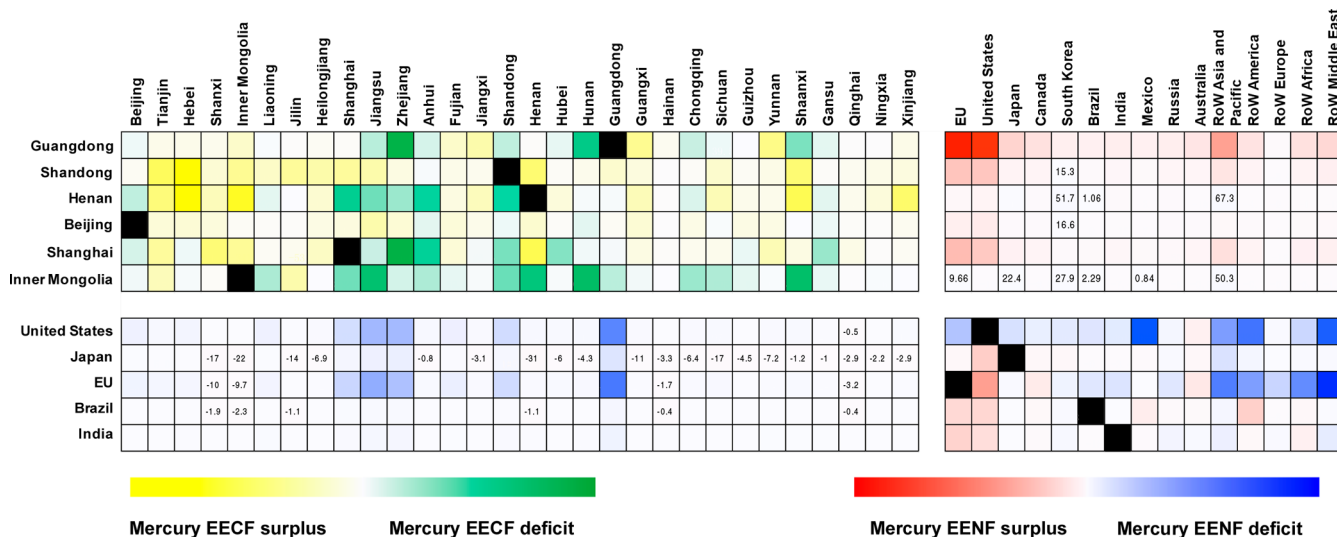
Figure 3. Mercury emissions embodied in the trade of final products.

the 30 Chinese provinces, Henan, Shandong, Gansu, Yunnan, and Jiangsu are the top 5 provinces with the highest mercury PBI. Shandong and Jiangsu are the top 2 provinces for both mercury FBI and CBI. Shandong and Jiangsu emitted 54 and 50 t of FBI, respectively, and 46 and 39 t of CBI, respectively. Although the mercury FBI and CBI of Shandong were higher than those of other provinces, both were lower than the PBI of Shandong. Specifically, the mercury FBI and CBI of this province were 1.4% and 16.8% lower than the Shandong mercury PBI. A similar situation can be found in Henan, Gansu, Hunan, and Shaanxi. The possible reason for such observation is that these provinces produces more primary products as intermediate inputs for other regions, coinciding with the fact that the mercury-related production activities of these provinces are mainly located in upstream of the global supply chain. Especially in Henan province, the mercury PBI of Henan was 40% and 43% higher than the mercury FBI and CBI of this province, respectively. In contrast, the FBI and CBI values of Guangdong, Zhejiang, Shanghai, and Beijing were higher than their corresponding PBI values. These provinces are the most developed areas in China and play important roles as final producers and consumers in the global economic supply chain. Meanwhile, the mercury FBI values of these provinces were higher than their mercury CBI values, meaning that the production of mercury-intensive final products to be consumed in other global regions is larger than the production of mercury-intensive primary products for other global regions and the consumption of mercury-intensive final products from other global regions.

In terms of the world scope, the mercury PBI, FBI, and CBI of global countries and regions are shown in Figure 2b. Analogous to a previous study by Liang et al.,[20] for some non-Annex B countries (e.g., China, Brazil), the mercury CBI was lower than the mercury PBI and FBI. For some developed Annex B countries (e.g., E.U., U.S.A., and Japan), the mercury CBI was higher than the mercury PBI and FBI. Considering Chinese province as individual economic entity, the province in China with the highest mercury PBI, Henan, contributed 3.4% of the total global mercury PBI. This value was slightly lower than that of the E.U. (4.6%) and Turkey (3.9%) but higher than that of the U.S.A. (2.9%), India (2.0%), Australia (1.1%), and Japan (0.9%). The mercury PBI of Shandong

(2.9%), Gansu (2.3%), and Yunnan (2.3%) was approximately equivalent to that of the U.S.A. The mercury FBI values of the E.U. and U.S.A., however, were 8.7% and 5.3% of the total global emissions, respectively, exceeding the highest mercury FBI province, Shandong (2.9%), in China. The same situation was observed for the mercury CBI. The E.U. and U.S.A. contributed 10.16% and 6.89% of the total global mercury CBI, respectively. The province in China with the highest mercury CBI was Shandong (2.4%). The mercury PBIs of some other countries (e.g., Japan, South Korea, India, and Australia) were lower than those of many Chinese provinces. For example, South Korea contributed 0.4% of the total global mercury PBI, which exceeded the mercury PBI of 7 provinces in China. However, South Korea contributed 1.1% of the total global mercury FBI and 1.0% of the total global mercury CBI; these values were higher than those of 21 and 18 provinces in China, respectively. The mercury FBI (1.8%) and CBI (1.9%) of Japan were equivalent to those of Henan and Shandong, but the mercury PBI of Japan (0.9%) was far less than that of Henan and Shandong.

Meanwhile, Figure S4 exhibits the per capita mercury footprint of Chinese provinces and other countries. The average per capita mercury footprint of China was 0.45 g per person per year and was followed by the footprint of the U.S.A. (0.44 g/p), Canada (0.40 g/p), and E.U. (0.38 g/p). Tianjin had the highest mercury footprint per person (0.95 g/p) among all Chinese provinces and other countries. Australia had the highest mercury footprint per person (0.94 g/p) among other countries, with a value slightly lower than that of Tianjin and higher than that of Shanghai (0.88 g/p) and Ningxia (0.81 g/p). The richer regions in China, such as Shanghai, Beijing, Zhejiang, and Jiangsu, had the highest mercury footprint per person. The mercury footprint per person of these provinces was equivalent or slightly higher than that in some countries, such as Norway, Brazil, and Turkey, and higher than that in most countries and regions of the world. The international share of the per capita mercury footprint varied from 0.5% (Gansu) to 2.7% (Fujian), while the interprovince share of the per capita mercury footprint varied from 3.2% (Gansu) to 49.1% (Tianjin).

Mercury Emissions Embodied in Final Products Trade (FT) and Intermediate Products Trade (IT). In the analysis

E

of emissions embodied in trade, Chinese provinces are regarded as individual trading entities, equivalent to other countries. We found a total of 304 t of mercury emissions embodied in FT, of which 203 t (66.8%) were embodied in international final products trade (NFT) and 101 t (33.2%) were embodied in China interprovince final products trade (RFT). Guangdong had the largest amount of international final products exports (NFTE) embodied mercury emissions of all Chinese provinces (12.5 t), which accounted for 27.0% of the total mercury emissions embodied in Chinese NFTE. Henan has the largest amount of interprovince final product exports (RFTE) embodied mercury emissions (9.9 t), which accounted for 9.7% of the total mercury emissions embodied in China RFT. The major NFTE-embodied mercury emissions occurred in the east coast provinces of China (e.g., Guangdong, Jiangsu, Zhejiang, Shandong, Shanghai) (Figure S2A). The amount of these provinces was 40 t, accounting for 86% of the total. The eastern coastal regions are the main contributors to Chinese GDP. These provinces have more international trade final goods production activities than other inner mainland provinces. In contrast, the mercury emissions embodied in China RFTE were similar among provinces. Over two-thirds of the provinces had over 1 t of embodied mercury emissions. In terms of imports, as shown in Figure S2C, the total mercury emissions embodied in international final products exports (NFTI) were 80% lower than the NFTE-embodied mercury emissions. NFTI-embodied mercury emissions ranged from 0.03 t in Qinghai to 0.83 t in Shandong. Henan also had the largest amount of interprovince final products imports trade (RFTI)-embodied mercury emissions (8.1 t), and the performance of RFTI-embodied mercury emissions was similar to that of RFTE-embodied mercury emissions.

The upper panel of Figure 3 show the mercury emissions embodied in the Chinese interprovince and international final products trading of 6 representative provinces: Guangdong, Shandong, Henan, Beijing, Shanghai, and Inner Mongolia. Guangdong province exhibited a high mercury EENF surplus to all international trade countries and regions. The embodied mercury emissions surpluses in NFT between Guangdong and E.U. and the U.S.A. were 3.2 and 2.9 t, respectively. Compared to the high embodied mercury emissions export in NFT, the embodied mercury emissions export in RFT of Guangdong with all other provinces was less than 1 t, showing a mercury EECF deficit with most provinces. Guangdong is the largest Chinese international trade producer. It produces a large amount of final goods used for international exports. The mercury-intensive final products of this province are mainly exported to other countries, such as the E.U., the U.S.A., Japan, and R.A.P., but are not consumed in other Chinese provinces. Analogously, Shandong (a large province in China) and Beijing (municipality and the capital of China) showed high embodied mercury EENF surplus but both had embodied mercury EENF deficits with South Korea. Different from Guangdong province, Shandong and Beijing also showed a mercury EECF surplus with other provinces. Henan, Inner Mongolia, and Shanghai, showed high mercury EECF deficits. The mercury emissions embodied in NFT were very low for Inner Mongolia, owing to its inland location in China.

At the world scope, the E.U. is the largest export destination for embodied mercury emissions from Chinese provinces. Most Chinese provinces show mercury EENF surplus with the E.U. Guangdong, Jiangsu, Zhejiang, Shanghai, and Shandong

contributed 9.2 t of export-embodied mercury emissions to the E.U., comprising 20% of the total E.U. import-embodied mercury emissions. The U.S.A. was the second largest export-embodied mercury emissions destination. Meanwhile, Japan was the largest import-embodied mercury emissions source of Chinese provinces (Shown in the bottom panel of Figure 3). This Asian country shows mercury EENF surplus with most Chinese provinces. Its import-embodied mercury emissions were distributed to all Chinese provinces equally.

The global mercury emissions embodied in IT were calculated to be 907 t, 66.5% higher than the embodied mercury emissions in FT. For China, there were 83 t of mercury emissions embodied in international intermediate products exports (NITE), and 54 t of mercury emissions were embodied in international intermediate products imports (NITI). Compared to the emissions embodied in NFT, the mercury emissions embodied in NITI of China were well above the mercury emissions embodied in NFTI of China. The net international export-embodied mercury emissions in the intermediate products trade was 29 t, which was less than the net international export-embodied mercury emissions in the final products trade (37t). That can be interpreted that China as world factory took on more trade in intermediated mercury-intensive products.

The comparison of the trade balance of the embodied mercury emissions in the trade of final and intermediate products of 30 provinces in China is given in Figure S3. We also differentiated international and interprovince trades. We observed that most provinces, except for Inner Mongolia, Shanxi, Qinghai, and Hainan, were net exporters of embodied mercury emissions in NFT (Figure S3a). Nonetheless, the embodied mercury emissions of net imports for the international trade of final products in these four provinces were low and less than 0.1 t. This result means that almost all provinces were net exporters for embodied mercury emissions in NFT. However, more provinces were net importers for embodied mercury emissions in NIT (e.g., Jiangxi, Anhui, Hebei, Inner Mongolia, etc.) (Figure S3a). This result means that most provinces imported intermediate mercury-intensive products from other countries to satisfy production activities. For interprovince trade, the eastern developed provinces (e.g., Guangdong, Zhejiang, Jiangsu, and Shanghai) needed to import intermediate mercury-intensive products from other provinces. These eastern provinces were net importers of embodied mercury emissions in RIT. During manufacturing activities, these mercury-intensive products are further processed to final products and traded to other provinces. Thus, these products have high embodied mercury emissions in RFT (Figure S3b).

Uncertainty. Uncertainties in the footprints result from uncertain mercury emissions inventory and the nested MRIO tables. For greenhouse gas emissions, it has been found that divergences in emissions inventories are the more important source for the divergence in national consumption-based accounts among MRIO databases, while the economic modeling introduces a significant uncertainty at the level of individual products.[60] Due to unavailability of international trade data of individual Chinese provinces to other countries, we assumed that the sectoral structure of Chinese provincial foreign trade destination is the same as the sectoral structure of China's national foreign trade. Chinese provincial trade to other countries may deviates very much from our allocation as sectoral structure varies due to geographical location and

nonhomogenous product groups, affecting the results to a certain extent. To simulate and propagate the before mentioned and unforeseen uncertainties, we have used Monte Carlo simulation method. Uncertainty ranges of PBI, FBI and CBI are presented as 95% confidence intervals in Figure 1. In general, uncertainty of Chinese province mercury footprint vary from 8% to 34%. The high uncertainty value was observed in Gansu (34%). Also, the distribution of the simulated mercury emissions multipliers varies by sectors and regions. We found the uncertainties of 8−234% for all individual product sectors mercury multipliers. The representative simulation results are presented in Figure 4. It shows that
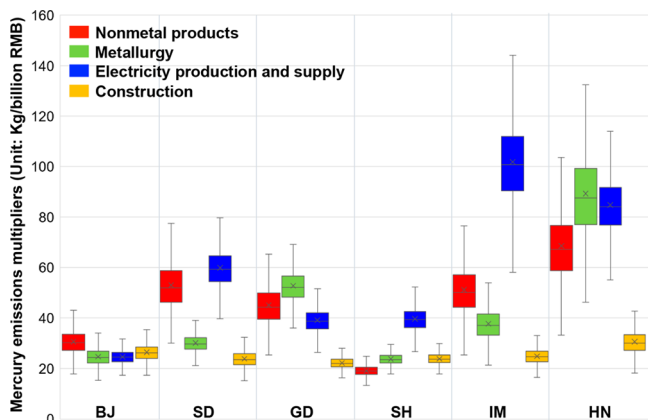
Figure 4. The distribution of Monte Carlo simulated results for mercury emissions multipliers of key sectors in representative provinces. BJ: Beijing; SD: Shandong; GD: Guangdong; SH: Shanghai; IM: Inner Mongolia; and HN: Henan.

uncertainties of mercury emission multipliers of sectors in Inner Mongolia and Henan were higher than that in Beijing and Shanghai (seen in Figure 4 and Table S2). The electricity production and supply sector in Inner Mongolia has the highest distribution of mercury emissions multipliers than other sectors (Figure 4). Gansu has the both metallurgy and construction sectors with the highest mercury emission multipliers, with uncertainty exceeding to 40% (Table S2). Compared to Chinese province and other countries, the sectors in Chinese province show the higher uncertainties. Note also, the sectors with the lower mercury emissions multipliers show higher uncertainties. The same trend of lower mercury emissions sectors showing higher uncertainties (RSDs) also appears in sectorial final consumptions. As shown in Figure S7, while the quantities of sectorial final consumptions increase, the logarithm of RSDs decreases for both the selected six Chinese provinces and other regions.

Uncertainties may also be caused by the choice of Chinese and international MRIO database.[61] We estimated and compared the uncertainties associated with the choice of Chinese MRIO in nested input−output model from three various Chinese MRIO tables. These tables were named by the developed groups (e.g., ISDCAS,[62,63] NUAA,[64] and CEADs[65,66]). The uncertainties for Chinese individual sectors mercury emissions multipliers of ISDCAS, NUAA, and CEADs range from 10%−232%, 9%−138%, and 10%−126%, respectively. In addition, comparative study of emission multipliers of the nested MRIO table and nested MRIO tables generated from the other three Chinese MRIO tables shows that the difference in magnitude generally scattered within [−1,1],

while only ISDCAS shows a difference in magnitude of 2 in Chinse construction sectors. Results show there are uncertainty differences occurred in the various Chinese MRIO tables and robust footprint researches would rely on the suitable and steady MRIO tables.

Limitations and Policy Implications. Mercury emission reductions is a global challenge, and some joint efforts, such as the "Minamata Convention on Mercury", have been conducted by international society. China, as the largest mercury emitter, plays a vital role in mercury emission reductions. The existence of large spatial heterogeneity in China makes mercury footprint analysis at the subnational level an important tool to help the Chinese government formulate effective mercury control policies. Hence, we used the nested China-global MRIO model in this study to investigate the Chinese provincial mercury footprint within the global supply chain. Compared to previous studies that investigated the mercury footprint of nations based on a global-scale MRIO model[20,25] or the Chinese mercury footprint based on a Chinese national-scale MRIO model,[26] our analysis provided a more comprehensive account of Chinese provincial mercury pollution considering impacts from global supply chains.

Reducing global mercury emissions requires not only the responsibilities of countries to be clarified but also emissions to be addressed at the subnational level. Understanding the Chinese provincial mercury footprint within the global supply chain can facilitate the adoption of concrete and effective actions for mercury emission reductions. In order to implement Minamata Convention nationally, the Ministry of Ecology and Environment of China has introduced several high-level plans. In the recent speech[67] delivered by Vice Minister Zhao Yingmin on the anniversary of Minamata Convention rectification in China, he summarized the Chinese national plan to reduce mercury emission by supply side measures such as tightening mercury emission license issuance in key polluting industries, improving monitoring and law enforcement, and formulating policies that follows BAT/BEP principles. However, due to the complexity of mercury emission shown in our research, it would be less effective to curtail mercury emission with one single set of regulations. Regional specific policies should be devised based on the emission characteristics. For example, it has already been identified in Minister Zhao's speech that metal smelting, electricity, and heat power are the key focus of supply side mercury emission reduction, agreeing with our finding. To act as a guidance for law enforcement and monitoring emphasis, our research implies that more resources on law enforcement should be directed to western and inland provinces such as Yunnan and Gansu for better impacts.

On the contrary, demand side policies should also be implemented in regions where final product consumption induces more mercury emissions. For example, Jiangsu and Shandong have the highest FBI, suggesting final product consumption in these two provinces induces higher mercury emissions. Hence, policies on mercury containing waste (e.g., fluorescent lamps) recycling should be the emphasis in these regions. Currently, minimum effort has been made in the recycling of household consumed mercury containing wastes.[68] With reference to our study, Chinese high-level advising institution and think tanks (e.g., Chinese Academy of Environment Planning, Chinese Research Academy of Environmental Sciences) could formulate policy recommendations for the Ministry of Ecology and Environment as well as

the Central Government on where to launch the most effective household mercury containing wastes recycling scheme to ensure economic-of-scale for sorting and recycling stations. Since the Chinese government relies more on top-down designs for policy devising, we believe such a macro-level accounting research could facilitate the Central Government to initiate effective measures to curtail mercury emission from demand side perspectives too.

Last but not least, we would also like to point out that studies of nesting national MRIOs into global MRIOs is at its early stage. Due to information gaps in raw data used, uncertainties are propagated in the nesting process. When using our results as a reference for policy making, one should be aware that the accounted amount of mercury emissions is prone to inherited uncertainties from the construction of MRIO tables used. Hence, best and worst scenarios of emissions should be quoted if our result is to be used for policy recommendation report formulation. If uncertainties from MRIO tables used could be reduced from the database builders' end, then uncertainties propagated from the nesting process could be vastly decreased. In addition, spatially explicit MRIO tables could be developed to further analyze internationally extended mercury footprints or even other environmental footprints of subcountry regions or cities in other countries with larger demographic and geographic sizes, such as India and the U.S.A. By nesting the MRIO tables of larger economies with global MRIO table, researchers, and policy makers could investigate the embodied flow of emissions at an unprecedentedly high resolution, so that they could collaborate more effectively toward emission mitigations.

■ ASSOCIATED CONTENT

ⓢ Supporting Information

Supporting Information 1 and 2 The Supporting Information is available free of charge on the ACS Publications website at DOI: 10.1021/acs.est.8b06373.

Text S1. Detailed materials and methods; Text S2. supplemental results; Text S3. uncertainty analysis for the nested MRIO and choice of Chinese MRIO tables; (Tables S1−S6 and Figures S1−S7) (PDF)

EXIOBASE20p_CC30 data (XLSX)

■ AUTHOR INFORMATION

Corresponding Authors
*Phone: +86-1062759190; e-mail: xjwang@urban.pku.edu.cn (X.W.).
*Phone: +1-2034325475; e-mail: edgar.hertwich@yale.edu (E.H.).

ORCID ⓘ
Haoran Zhang: 0000-0002-8751-5407
Kehan He: 0000-0002-8553-0048
Xuejun Wang: 0000-0001-9990-1391
Edgar G. Hertwich: 0000-0002-4934-3421

Author Contributions
§These authors contributed equally to this work.

Notes
The authors declare no competing financial interest.

■ ACKNOWLEDGMENTS

■ REFERENCES

(1) Tukker, A.; Bulavskaya, T.; Giljum, S.; de Koning, A.; Lutter, S.; Simas, M.; Stadler, K.; Wood, R. Environmental and resource footprints in a global context: Europe's structural deficit in resource endowments. *Global Environ. Chang* **2016**, *40*, 171−181.

(2) Weinzettel, J.; Steen-Olsen, K.; Hertwich, E. G.; Borucke, M.; Galli, A. Ecological footprint of nations: Comparison of process analysis, and standard and hybrid multiregional input-output analysis. *Ecol Econ* **2014**, *101*, 115−126.

(3) Krausmann, F.; Erb, K. H.; Gingrich, S.; Haberl, H.; Bondeau, A.; Gaube, V.; Lauk, C.; Plutzar, C.; Searchinger, T. D. Global human appropriation of net primary production doubled in the 20th century. *Proc. Natl. Acad. Sci. U. S. A.* **2013**, *110* (25), 10324−10329.

(4) Lutter, S.; Giljum, S.; Bruckner, M. A review and comparative assessment of existing approaches to calculate material footprints. *Ecol Econ* **2016**, *127*, 1−10.

(5) Giljum, S.; Bruckner, M.; Martinez, A. Material Footprint Assessment in a Global Input-Output Framework. *J. Ind. Ecol.* **2015**, *19* (5), 792−804.

(6) Creutzig, F.; Roy, J.; Lamb, W. F.; Azevedo, I. M. L.; de Bruin, W. B.; Dalkmann, H.; Edelenbosch, O. Y.; Geels, F. W.; Grubler, A.; Hepburn, C.; Hertwich, E. G.; Khosla, R.; Mattauch, L.; Minx, J. C.; Ramakrishnan, A.; Rao, N. D.; Steinberger, J. K.; Tavoni, M.; Urge-Vorsatz, D.; Weber, E. U. Towards demand-side solutions for mitigating climate change. *Nat. Clim. Change* **2018**, *8* (4), 260−263.

(7) Peters, G. P. Carbon footprints and embodied carbon at multiple scales. *Curr. Opin Sust* **2010**, *2* (4), 245−250.

(8) Wiedmann, T.; Lenzen, M. Environmental and social footprints of international trade. *Nat. Geosci.* **2018**, *11* (5), 314−321.

(9) Lenzen, M.; Sun, Y. Y.; Faturay, F.; Ting, Y. P.; Geschke, A.; Malik, A. The carbon footprint of global tourism. *Nat. Clim. Change* **2018**, *8* (6), 522−528.

(10) Malik, A.; Lenzen, M.; McAlister, S.; McGain, F. The carbon footprint of Australian health care. *Lancet Planet Health* **2018**, *2* (1), e27−e35.

(11) Wiedenhofer, D.; Guan, D. B.; Liu, Z.; Meng, J.; Zhang, N.; Wei, Y. M. Unequal household carbon footprints in China. *Nat. Clim. Change* **2017**, *7* (1), 75−80.

(12) Wang, R. R.; Zimmerman, J. Hybrid Analysis of Blue Water Consumption and Water Scarcity Implications at the Global, National, and Basin Levels in an Increasingly Globalized World. *Environ. Sci. Technol.* **2016**, *50* (10), 5143−5153.

(13) Wiedmann, T. O.; Schandl, H.; Lenzen, M.; Moran, D.; Suh, S.; West, J.; Kanemoto, K. The material footprint of nations. *Proc. Natl. Acad. Sci. U. S. A.* **2015**, *112* (20), 6271−6276.

(14) Steen-Olsen, K.; Wood, R.; Hertwich, E. G. The Carbon Footprint of Norwegian Household Consumption 1999−2012. *J. Ind. Ecol.* **2016**, *20* (3), 582−592.

(15) Chen, B.; Li, J. S.; Wu, X. F.; Han, M. Y.; Zeng, L.; Li, Z.; Chen, G. Q. Global energy flows embodied in international trade: A combination of environmentally extended input-output analysis and complex network analysis. *Appl. Energy* **2018**, *210*, 98−107.

(16) Chen, B.; Han, M. Y.; Peng, K.; Zhou, S. L.; Shao, L.; Wu, X. F.; Wei, W. D.; Liu, S. Y.; Li, Z.; Li, J. S.; Chen, G. Q. Global land-water nexus: Agricultural land and freshwater use embodied in worldwide supply chains. *Sci. Total Environ.* **2018**, *613*, 931−943.

(17) Peters, G. P.; Hertwich, E. G. CO2 embodied in international trade with implications for global climate policy. *Environ. Sci. Technol.* **2008**, *42* (5), 1401−1407.

(18) Oita, A.; Malik, A.; Kanemoto, K.; Geschke, A.; Nishijima, S.; Lenzen, M. Substantial nitrogen pollution embedded in international trade. *Nat. Geosci.* **2016**, *9* (2), 111−115.

(19) Kanemoto, K.; Moran, D.; Hertwich, E. G. Mapping the Carbon Footprint of Nations. *Environ. Sci. Technol.* **2016**, *50* (19), 10512−10517.

(20) Liang, S.; Wang, Y. F.; Cinnirella, S.; Pirrone, N. Atmospheric Mercury Footprints of Nations. *Environ. Sci. Technol.* **2015**, *49* (6), 3566−3574.

(21) AMAP/UNEP. *Technical Background Report for the Global Mercury Assessment 2013*; Arctic Monitoring and Assessment Programme: Oslo, Norway/UNEP Chemicals Branch: Geneva, Switzerland, 2013.

(22) Zhang, H. R.; Chen, L.; Tong, Y. D.; Zhang, W.; Yang, W.; Liu, M. D.; Liu, L. B.; Wang, H. H.; Wang, X. J. Impacts of supply and consumption structure on the mercury emission in China: An input-output analysis based assessment. *J. Cleaner Prod.* **2018**, *170*, 96−107.

(23) Lin, Y.; Wang, S. X.; Wu, Q. R.; Larssen, T. Material Flow for the Intentional Use of Mercury in China. *Environ. Sci. Technol.* **2016**, *50* (5), 2337−2344.

(24) Zhang, L.; Wang, S. X.; Wang, L.; Wu, Y.; Duan, L.; Wu, Q. R.; Wang, F. Y.; Yang, M.; Yang, H.; Hao, J. M.; Liu, X. Updated Emission Inventories for Speciated Atmospheric Mercury from Anthropogenic Sources in China. *Environ. Sci. Technol.* **2015**, *49* (5), 3185−3194.

(25) Li, J. S.; Chen, B.; Chen, G. Q.; Wei, W. D.; Wang, X. B.; Ge, J. P.; Dong, K. Q.; Xia, H. H.; Xia, X. H. Tracking mercury emission flows in the global supply chains: A multi-regional input-output analysis. *J. Cleaner Prod.* **2017**, *140*, 1470−1492.

(26) Liang, S.; Zhang, C.; Wang, Y. F.; Xu, M.; Liu, W. D. Virtual Atmospheric Mercury Emission Network in China. *Environ. Sci. Technol.* **2014**, *48* (5), 2807−2815.

(27) Hui, M. L.; Wu, Q. R.; Wang, S. X.; Liang, S.; Zhang, L.; Wang, F. Y.; Lenzen, M.; Wang, Y. F.; Xu, L. X.; Lin, Z. T.; Yang, H.; Lin, Y.; Larssen, T.; Xu, M.; Hao, J. M. Mercury Flows in China and Global Drivers. *Environ. Sci. Technol.* **2017**, *51* (1), 222−231.

(28) Chen, L.; Meng, J.; Liang, S.; Zhang, H. R.; Zhang, W.; Liu, M. D. A.; Tong, Y. D.; Wang, H. H.; Wang, W.; Wang, X. J.; Shu, J. Trade-Induced Atmospheric Mercury Deposition over China and Implications for Demand-Side Controls. *Environ. Sci. Technol.* **2018**, *52* (4), 2036−2045.

(29) Lenzen, M.; Kanemoto, K.; Moran, D.; Geschke, A. Mapping the Structure of the World Economy. *Environ. Sci. Technol.* **2012**, *46* (15), 8374−8381.

(30) Lenzen, M.; Moran, D.; Kanemoto, K.; Geschke, A. Building Eora: A Global Multi-Region Input-Output Database at High Country and Sector Resolution. *Econ Syst. Res.* **2013**, *25* (1), 20−49.

(31) Wood, R.; Stadler, K.; Bulavskaya, T.; Lutter, S.; Giljum, S.; de Koning, A.; Kuenen, J.; Schutz, H.; Acosta-Fernandez, J.; Usubiaga, A.; Simas, M.; Ivanova, O.; Weinzettel, J.; Schmidt, J. H.; Merciai, S.; Tukker, A. Global Sustainability Accounting-Developing EXIOBASE for Multi-Regional Footprint Analysis. *Sustainability* **2015**, *7* (1), 138−163.

(32) Aguiar, A.; Narayanan, B.; McDougall, R. An Overview of the GTAP 9 Data Base. *J. Glob Econ Anal* **2016**, *1* (1), 181−208.

(33) Dietzenbacher, E.; Los, B.; Stehrer, R.; Timmer, M.; de Vries, G. The Construction of World Input-Output Tables in the Wiod Project. *Econ. Syst. Res.* **2013**, *25* (1), 71−98.

(34) Wiebe, K. S.; Bruckner, M.; Giljum, S.; Lutz, C. Calculating Energy-Related Co2 Emissions Embodied in International Trade Using a Global Input-Output Model. *Econ Syst. Res.* **2012**, *24* (2), 113−139.

(35) Wiebe, K. S.; Bruckner, M.; Giljum, S.; Lutz, C.; Polzin, C. Carbon and Materials Embodied in the International Trade of Emerging Economies A Multiregional Input-Output Assessment of Trends Between 1995 and 2005. *J. Ind. Ecol.* **2012**, *16* (4), 636−646.

(36) Davis, S. J.; Caldeira, K. Consumption-based accounting of CO2 emissions. *Proc. Natl. Acad. Sci. U. S. A.* **2010**, *107* (12), 5687−5692.

(37) Feng, K. S.; Davis, S. J.; Sun, L. X.; Li, X.; Guan, D. B.; Liu, W. D.; Liu, Z.; Hubacek, K. Outsourcing CO2 within China. *Proc. Natl. Acad. Sci. U. S. A.* **2013**, *110* (28), 11654−11659.

(38) Fry, J.; Lenzen, M.; Jin, Y. T.; Wakiyama, T.; Baynes, T.; Wiedmann, T.; Malik, A.; Chen, G. W.; Wang, Y. F.; Geschke, A.; Schandl, H. Assessing carbon footprints of cities under limited information. *J. Cleaner Prod.* **2018**, *176*, 1254−1270.

(39) Chen, G. Q.; Li, J. S.; Chen, B.; Wen, C.; Yang, Q.; Alsaedi, A.; Hayat, T. An overview of mercury emissions by global fuel combustion: The impact of international trade. *Renewable Sustainable Energy Rev.* **2016**, *65*, 345−355.

(40) Christis, M.; Geerken, T.; Vercalsteren, A.; Vrancken, K. C. Improving footprint calculations of small open economies: combining local with multi-regional input-output tables. *Econ Syst. Res.* **2017**, *29* (1), 25−47.

(41) Wang, Y. F.; Geschke, A.; Lenzen, M. Constructing a Time Series of Nested Multiregion Input-Output Tables. *Int. Regional Sci. Rev.* **2017**, *40* (5), 476−499.

(42) Liu, Z.; Davis, S. J.; Feng, K.; Hubacek, K.; Liang, S.; Anadon, L. D.; Chen, B.; Liu, J. R.; Yan, J. Y.; Guan, D. B. Targeted opportunities to address the climate-trade dilemma in China. *Nat. Clim. Change* **2016**, *6* (2), 201−206.

(43) Lenzen, M.; Wood, R.; Wiedmann, T. Uncertainty Analysis for Multi-Region Input-Output Models - a Case Study of the Uk's Carbon Footprint. *Econ Syst. Res.* **2010**, *22* (1), 43−63.

(44) Peters, G. P. From production-based to consumption-based national emission inventories. *Ecol Econ* **2008**, *65* (1), 13−23.

(45) Liang, S.; Wang, Y. F.; Zhang, C.; Xu, M.; Yang, Z. F.; Liu, W. D.; Liu, H. G.; Chiu, A. S. F. Final production-based emissions of regions in China. *Econ Syst. Res.* **2018**, *30* (1), 18−36.

(46) Peters, G. H. E. G. *Production Factors and Pollution Embodied in Trade: Theoretical Development*; Norwegian University of Science and Technology: Norway, 2004.

(47) Miller, R. E. B. P.D. *Input−Output Analysis: Foundations and Extensions*, 2ⁿᵈ ed.; Cambridge University Press: Cambridge, 2009.

(48) Kanemoto, K.; Lenzen, M.; Peters, G. P.; Moran, D. D.; Geschke, A. Frameworks for Comparing Emissions Associated with Production, Consumption, And International Trade. *Environ. Sci. Technol.* **2012**, *46* (1), 172−179.

(49) Hertwich, E. G.; Wood, R. The growing importance of scope 3 greenhouse gas emissions from industry. *Environ. Res. Lett.* **2018**, *13* (10), 104013.

(50) Wu, X. F.; Chen, G. Q. Global primary energy use associated with production, consumption and international trade. *Energy Policy* **2017**, *111*, 85−94.

(51) Guan, D. B.; Su, X.; Zhang, Q.; Peters, G. P.; Liu, Z.; Lei, Y.; He, K. B., The socioeconomic drivers of China's primary PM2.5 emissions. *Environ. Res. Lett.* **2014**, *9* (2), 024010.

(52) Zheng, X. Z.; Wang, R. R.; Wood, R.; Wang, C.; Hertwich, E. G. High sensitivity of metal footprint to national GDP in part explained by capital formation. *Nat. Geosci.* **2018**, *11* (4), 269.

(53) Stadler, K.; Wood, R.; Bulavskaya, T.; Sodersten, C. J.; Simas, M.; Schmidt, S.; Usubiaga, A.; Acosta-Fernandez, J.; Kuenen, J.; Bruckner, M.; Giljum, S.; Lutter, S.; Merciai, S.; Schmidt, J. H.; Theurl, M. C.; Plutzar, C.; Kastner, T.; Eisenmenger, N.; Erb, K. H.; de Koning, A.; Tukker, A. EXIOBASE 3: Developing a Time Series of Detailed Environmentally Extended Multi-Regional Input-Output Tables. *J. Ind. Ecol.* **2018**, *22* (3), 502−515.

(54) Liu, W. D. T. Z. P.; Chen, J.; Yang, B. *China's Interregional Input−Output Table for 30 Regions in 2010 (in Chinese)*; China Statistics Press: Beijing, China, 2014.

(55) Rodrigues, J. F. D.; Moran, D.; Wood, R.; Behrens, P. Uncertainty of Consumption-Based Carbon Accounts. *Environ. Sci. Technol.* **2018**, *52* (13), 7577−7586.

(56) Hertwich, E. G.; Peters, G. P. Carbon Footprint of Nations: A Global, Trade-Linked Analysis. *Environ. Sci. Technol.* **2009**, *43* (16), 6414−6420.

(57) Bullard, C. W.; Sebald, A. V. Monte-Carlo Sensitivity Analysis of Input-Output Models. *Rev. Econ Stat* **1988**, *70* (4), 708−712.

(58) Bullard, C. W., III; Sebald, A. V. Effects of parametric uncertainty and technological change on input-output models. *Review of Economics and Statistics LIX* **1977**, *59* (1), 75−81.

(59) Quandt, R. E. Probabilistic errors in the Leontief system. *Naval Research Logistics Quarterly* **1958**, *5*, 155−170.

(60) Moran, D.; Kanemoto, K. Tracing global supply chains to air pollution hotspots. *Environ. Res. Lett.* **2016**, *11* (9), 094017.

(61) Tukker, A.; de Koning, A.; Owen, A.; Lutter, S.; Bruckner, M.; Giljum, S.; Stadler, K.; Wood, R.; Hoekstra, R. Towards Robust, Authoritative Assessments of Environmental Impacts Embodied in Trade: Current State and Recommendations. *J. Ind. Ecol.* **2018**, *22* (3), 585−598.

(62) Zhang, W.; Liu, Y.; Feng, K. S.; Hubacek, K.; Wang, J. N.; Liu, M. M.; Jiang, L.; Jiang, H. Q.; Liu, N. A. L.; Zhang, P. Y.; Zhou, Y.; Bi, J. Revealing Environmental Inequality Hidden in China's Inter-regional Trade. *Environ. Sci. Technol.* **2018**, *52* (13), 7171−7181.

(63) Zhang, W.; Wang, F.; Hubacek, K.; Liu, Y.; Wang, J. N.; Feng, K. S.; Jiang, L.; Jiang, H. Q.; Zhang, B.; Bi, J. Unequal Exchange of Air Pollution and Economic Benefits Embodied in China's Exports. *Environ. Sci. Technol.* **2018**, *52* (7), 3888−3898.

(64) Pan, C.; Peters, G. P.; Andrew, R. M.; Korsbakken, J. I.; Li, S. T.; Zhou, P.; Zhou, D. Q. Structural Changes in Provincial Emission Transfers within China. *Environ. Sci. Technol.* **2018**, *52* (22), 12958−12967.

(65) Mi, Z. F.; Meng, J.; Zheng, H. R.; Shan, Y. L.; Wei, Y. M.; Guan, D. B. A multi-regional input−output table mapping China's economic outputs and interdependencies in 2012. *Sci. Data* **2018**, *5*, 180155.

(66) Mi, Z. F.; Meng, J.; Guan, D. B.; Shan, Y. L.; Song, M. L.; Wei, Y. M.; Liu, Z.; Hubacek, K. Chinese CO_2 emission flows have reversed since the global financial crisis. *Nat. Commun.* **2017**, *8* DOI: 10.1038/s41467-017-01820-w.

(67) Zhao, Y. The speech at the meeting "To commemorate the minamata about mercury convention effect anniversary and the performance of China communication progress". In Chinese, M.o.E.a.E.o.t.P.s.R.o., Ed. 2018.

(68) Li, Z. G.; Jia, P. Q.; Zhao, F.; Kang, Y. K., Mercury Pollution, Treatment and Solutions in Spent Fluorescent Lamps in Mainland China. *Int. J. Environ. Res. Public Health* **2018**, *15* (12), 2766.